Pathological hypertrophy amelioration by PRAS40-mediated inhibition of mTORC1

Mirko Völkers[a,b], Haruhiro Toko[a,b], Shirin Doroudgar[a,b], Shabana Din[a,b], Pearl Quijada[a,b], Anya Y. Joyo[a,b], Luis Ornelas[a,b], Eri Joyo[a,b], Donna J. Thuerauf[a,b], Mathias H. Konstandin[a,b], Natalie Gude[a,b], Christopher C. Glembotski[a,b], and Mark A. Sussman[a,b,1]

[a]San Diego State University Heart Institute and the [b]Department of Biology, San Diego State University, San Diego, CA 92182

Edited by Eric N. Olson, University of Texas Southwestern Medical Center, Dallas, TX, and approved June 19, 2013 (received for review January 23, 2013)

Mechanistic target of rapamycin complex 1 (mTORC1), necessary for cellular growth, is regulated by intracellular signaling mediating inhibition of mTORC1 activation. Among mTORC1 regulatory binding partners, the role of Proline Rich AKT Substrate of 40 kDa (PRAS40) in controlling mTORC1 activity and cellular growth in response to pathological and physiological stress in the heart has never been addressed. This report shows PRAS40 is regulated by AKT in cardiomyocytes and that AKT-driven phosphorylation relieves the inhibitory function of PRAS40. PRAS40 overexpression in vitro blocks mTORC1 in cardiomyocytes and decreases pathological growth. Cardiomyocyte-specific overexpression in vivo blunts pathological remodeling after pressure overload and preserves cardiac function. Inhibition of mTORC1 by PRAS40 preferentially promotes protective mTORC2 signaling in chronic diseased myocardium. In contrast, strong PRAS40 phosphorylation by AKT allows for physiological hypertrophy both in vitro and in vivo, whereas cardiomyocyte-specific overexpression of a PRAS40 mutant lacking capacity for AKT-phosphorylation inhibits physiological growth in vivo, demonstrating that AKT-mediated PRAS40 phosphorylation is necessary for induction of physiological hypertrophy. Therefore, PRAS40 phosphorylation acts as a molecular switch allowing mTORC1 activation during physiological growth, opening up unique possibilities for therapeutic regulation of the mTORC1 complex to mitigate pathologic myocardial hypertrophy by PRAS40.

The mechanistic target of rapamycin (mTOR) kinase is a central cellular hub that couples nutrient sensing and growth factor signaling to cell growth and survival. mTOR signaling is often deregulated in cardiac diseases, and altered growth kinetics, metabolic changes, and increased susceptibility to cell death are characteristics of dysfunctional cardiomyocytes accumulating after cardiac damage. Pharmacological inhibition of mTORC1 with rapamycin improves cardiac function after pressure overload, myocardial infarction, and in genetic hypertrophic cardiomyopathies (1–3). Rapamycin improves cardiac function in patients after kidney transplantation and inhibits the development of cardiac hypertrophy (4), however no established therapeutic regime targets mTOR specifically in cardiomyocytes. As a consequence of the ubiquitous role of mTOR in cell biology, off-target and systemic effects limit clinical use of rapamycin in patients.

mTOR exists in two distinct complexes, mTORC1 and mTORC2 (5, 6). Regulatory-associated protein of mammalian target of rapamycin (Raptor) and Proline Rich AKT Substrate of 40 kDa (PRAS40) are specific to mTORC1. Although regulatory mechanisms activating mTORC1 are relatively well understood, those regulating mTORC2 are less characterized. mTORC2 is defined by assembly with rapamycin-insensitive companion of mTOR (Rictor) that has a regulatory role in the insulin signaling cascade and AKT activation (7). PRAS40 interacts with Raptor and inhibits mTORC1 kinase activity (8, 9). PRAS40 contains two proline-enriched stretches at the amino terminus and an AKT consensus phosphorylation site (RXRXXS/T) located at Thr246. Phosphorylated PRAS40 dissociates from mTORC1 in response to growth factors, insulin, glucose, and nutrients, thereby releasing the inhibitory function on mTORC1 (10, 11). Mutation of Thr246 to alanine inhibits AKT-mediated phosphorylation that is important to relieve the inhibitory action of PRAS40 on mTORC1 (9, 12). mTORC1 is an upstream regulator of PRAS40–Ser^{183} phosphorylation, which is important for binding of PRAS40 to Raptor (10, 11). PRAS40 regulates cellular growth and survival in vitro (13), but PRAS40 involvement in the regulation of growth in any tissue remains unexplored. As typical for other well-characterized regulators of cardiac growth and survival [e.g., AKT, proto-oncogene serine/threonine-protein kinase Pim-1 (PIM1), calcineurin], PRAS40 was initially discovered in noncardiac cells, but the relevance of PRAS40 in the myocardium has been overlooked. PRAS40 is widely expressed in various human and mouse tissues, with particularly high expression in the heart (14). In this study we demonstrate the cardioprotective effects of PRAS40-mediated inhibition of mTORC1 using a clinical relevant cardiac gene therapy.

Results

PRAS40 Is Expressed in Myocytes and Is Phosphorylated After Pressure Overload. PRAS40 is highly expressed in cardiomyocytes, with insulin treatment and subsequent AKT induction prompting PRAS40 phosphorylation at residues Thr^{246} and Ser^{183} together with activation of mTORC1 and mTORC2 (Fig. 1*A*).

PRAS40 is phosphorylated in response to insulin (Fig. 1*B*) and localized in the nucleus as shown by immunofluorescence, consistent with previous reports (15, 16). PRAS40 interaction with mTORC1 was assessed using proximity ligation assays (PLAs) in vitro. PRAS40 association with RAPTOR decreased after treatment with insulin (neonatal cardiomyocytes, NRCMs) in isolated neonatal myocytes and diminished binding of PRAS40 to mTOR after stimulation with insulin was confirmed by immunoprecipitation (Fig. S1*A*). The function of PRAS40 as an mTORC1 inhibitor can be negated by phosphorylation (thereby releasing mTORC1 inhibition) under conditions supporting increased mTORC1 activity, such as pressure overload induced by transaortic constriction (TAC). PRAS40 expression and phosphorylation were determined at multiple time points after TAC by immunoblot analysis. $PRAS^{T246}$ and $PRAS40^{S183}$ phosphorylation increased as early as 30 min after TAC (Fig. 1*C*), correlating with activation of mTORC1 as measured by phosphorylation of S6Kinase (S6K) as well as Ribosomal S6 protein (RibS6) and eukaryotic translation initiation factor 4E-binding protein 1 (4EBP) 4EBP, mTORC2 (measured by phosphorylation of AKT), and activation of fetal gene expression (Fig. S1*B*). PRAS40 phosphorylation diminished over time and decreased in the chronic phase of TAC response (5–8 wk postsurgery; Fig. 1*C*).

Author contributions: M.V., M.H.K., C.C.G., and M.A.S. designed research; M.V., H.T., S. Doroudgar, S. Din, P.Q., A.Y.J., L.O., E.J., D.J.T., and N.G. performed research; M.V. and C.C.G. analyzed data; and M.V. and M.A.S. wrote the paper.

The authors declare no conflict of interest.

This article is a PNAS Direct Submission.

[1]To whom correspondence should be addressed: E-mail: heartman4ever@icloud.com.

This article contains supporting information online at www.pnas.org/lookup/suppl/doi:10.1073/pnas.1301455110/-/DCSupplemental.

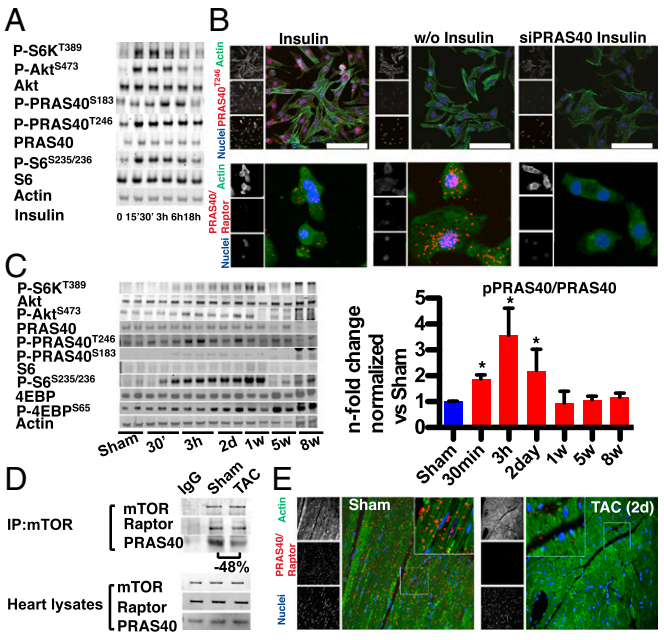

Fig. 1. PRAS40 is expressed in myocytes and is phosphorylated after pressure overload. (*A*) Time course after insulin stimulation. PRAS40 is phosphorylated after stimulation with insulin (100 nM). (*B*, *Upper*) Immunofluorescence of myocytes stained for pPRAS (red), actin (green), and nuclei (blue). PRAS40 is phosphorylated after insulin stimulation (20 min). Knockdown of PRAS40 with siRNA confirms specificity. (Scale bar, 150 μm.) (*B*, *Lower*) PLA (in red) in isolated myocytes under starvation conditions and after stimulation with insulin. Each red dot represents one interaction of PRAS40 with Raptor. Fewer interactions are present after insulin stimulation, indicating PRAS40 release from mTORC1. (*C*) Immunoblot showing a time course after TAC in 10-wk-old mice surgery for PRAS40 expression and phosphorylation. $*P < 0.05$ versus sham. (*D*) mTOR immunoprecipitation after sham or TAC surgery. (*E*) PLA in paraffin-embedded sections after TAC surgery. Fewer interactions are present after TAC, indicating PRAS40 release from mTORC1.

These data suggest that AKT-driven inactivation by phosphorylation of PRAS40 contributes early after TAC to activation of mTORC1. PRAS40 binding to mTOR decreased by 48% after TAC as assessed by immunoprecipitation (Fig. 1*D*). Decreased binding of PRAS40 to mTOR after pressure overload was confirmed by PLA in paraffin sections in vivo (Fig. 1*E*).

PRAS40 protein and phosphorylation levels were assessed in human failing myocardium using explanted cardiac tissue. PRAS40 protein expression was 2.1-fold higher together with increased PRAS40^{T246} phosphorylation in failing human myocardium relative to normal control myocardium, consistent with increased mTORC1 activation in failing hearts (Fig. S1*C*). Increased brain natriuretic peptide (BNP) levels confirmed failing myocardium (Fig. S1*C*).

PRAS40 Blocks Pathological Growth in Vitro. Because PRAS40 is an inhibitor of mTORC1, which is the major cellular regulator of growth, overexpression should block pathological hypertrophy. Therefore, the role of PRAS40 in hypertrophy was determined using adenoviral vectors carrying FLAG-tagged cDNAs encoding wild-type PRAS40 and a phospho-dead myc-tagged mutant (threonine to alanine, PRAS40TA). Consequences of PRAS40 overexpression for cardiomyocyte hypertrophy were examined using NRCMs infected with adenoviruses encoding PRAS40 or control followed by stimulation with phenylephrine (PE) for 24 h. PRAS40 phosphorylation did not significantly increase, indicating that PRAS40 phosphorylation is not required for the stimulation of mTORC1 signaling after PE, in line with previous reports (Fig. S2*A*) (17). PRAS40 overexpression inhibited PE-induced hypertrophy (Fig. 2 *A* and *B*) as assessed by cell surface area (CSA) measurements, comparable to the effect of rapamycin. As expected, the TA mutant blocked hypertrophic growth to a similar extent as the wild-type PRAS40 (Fig. 2*B*). mTOR kinase activity was inhibited in a dose-dependent manner by recombinant PRAS40 protein in vitro (Fig. 2*C*). Mechanistically, PRAS40 blocks increased mTORC1 (assessed by decreased phosphorylation of mTORC1 downstream targets S6K, RibS6, and 4EBP) activation in NRCM in response to PE (Fig. 2 *D* and *E*). The ratio of phosphorylated PRAS40–total PRAS40 was lower compared with control cells, which results in decreased mTORC1 activity in vitro (Fig. S2*A*). Expression of Raptor or phosphorylation of mTOR kinase remained unchanged after PRAS40 overexpression. Hypertrophic gene markers after PE showed decreased mRNA levels for atrial natriuretic peptide (ANP) by 91.3% and BNP by 52.4%, resulting from PRAS40 overexpression (Fig. S2*B*). To test if silencing of PRAS40 expression is sufficient to induce growth in NRCM, PRAS40-specific siRNAs were transfected into NRCMs. PRAS40 mRNA transcription was lowered to 9% of control levels within 48 h after silencing (Fig. S2*C*). Protein synthesis increased after PRAS40 silencing, which was associated with increased sensitivity to lower concentrations of PE and increased cellular size, whereas the maximal cell size was not affected after PRAS40 silencing (Fig. S2 *D* and *E*). Thus, PRAS40 overexpression blocks pathological hypertrophic growth in vitro by blocking mTORC1, whereas reduction of PRAS40 expression sensitizes cardiomyocytes to PE.

PRAS40 Blocks Pathological Growth in Vivo. An adeno-associated virus stereotype 9 (AAV9) virus expressing PRAS40 under regulatory control of myosin light chain (MLC) promoter in vivo was generated for cardiomyocyte-specific expression and to determine the effects of PRAS40 overexpression on pathological growth in vivo (Fig. S3*A*). PRAS40-overexpressing mice were then subjected to TAC. Staining for PRAS40 using the FLAG-tag confirmed overexpression in myocytes (Fig. S3*B*). Heart size was increased significantly in control mice at 1 and 5 wk after TAC (Fig. 3 *A* and *B*). Notably, hypertrophic growth was inhibited in hearts of PRAS40-overexpressing mice, as evidenced by a cross-sectional area of myocytes (Fig. 3*C*). PRAS40 blocked mTORC1 activation in response to TAC at 1 wk (Fig. 3*D*) as well as 5 wk after TAC (Fig. S3 *C* and *D*). Furthermore, molecular markers of hypertrophy such as ANP and BNP were induced after TAC in control mice after 1 wk (4.1-fold and 2.5-fold) and 5 wk (7.3-fold and 14.3-fold), but this increase was blocked in mice overexpressing PRAS40 (Fig. 3*E*). Consistent with blocked remodeling, PRAS40 TAC-challenged hearts exhibit decreased perivascular fibrosis and decreased collagen1 transcription (Fig. 3*F* and Fig. S3*D*) relative to their control TAC-challenged counterparts. Serial echocardiography was performed to measure cardiac function after TAC. Anterior wall thickening confirmed control hearts underwent remodeling starting 1 wk after challenge (Fig. 4*A* and Tables S1 and S2). In comparison, PRAS40 animals did not show significant increases in wall thickness up to 4 wk after surgery. In addition, left ventricular enlargement was completely prevented and systolic function preserved in PRAS40 animals (Fig. 4*B*).

PRAS40 Prevents Deterioration of Cardiac Function. Although the above results are a classic example of a prevention study, preemptive intervention does not reflect the clinical situation where patients most likely will be identified when they already have developed cardiac hypertrophy. To test the hypothesis that PRAS40 is protective when injected after banding when initiation of hypertrophy was confirmed by echocardiography, TAC mice were injected with PRAS40 or control virus 1 wk after banding (Fig. 5*A*). Hearts of control mice started to dilate and failed 4 wk after banding assessed with serial echocardiography. Cardiac function deteriorated for up to 8 wk after TAC in control animals,

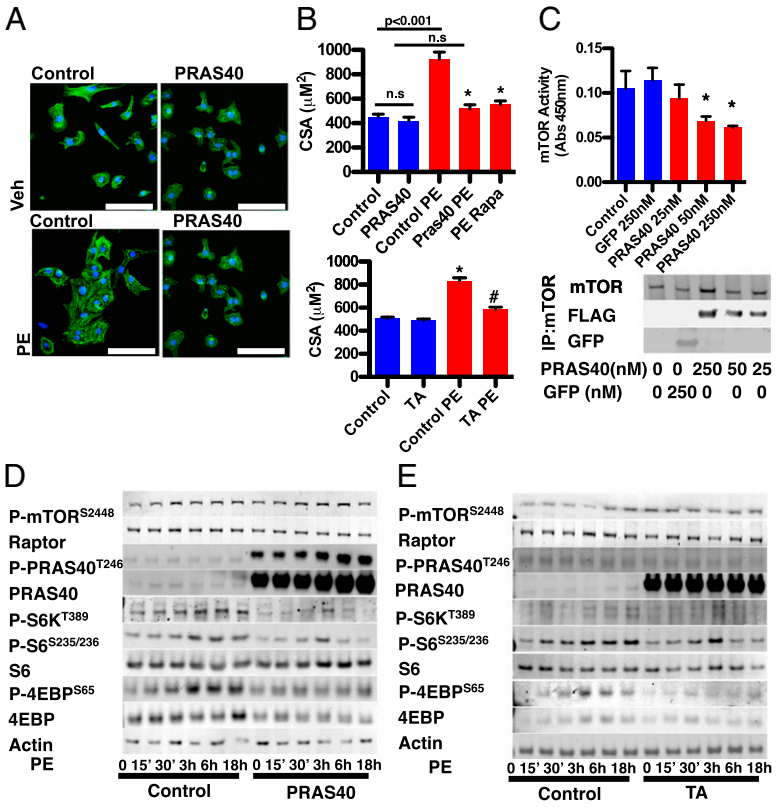

Fig. 2. PRAS40 blocks pathological growth in vitro. (*A*) Representative images of control and PRAS40-treated cardiac myocytes stained with an α-actinin antibody. Sytox is used as a stain for the nuclei. (Scale bar 150 μm.) (*B*) Individual CSA measurements from control, PRAS40, PRAS40TA, rapamycin-treated NRCMs, and those treated with PE (100 μM for 24 h) ($n = 4$ independent experiments, $^{*}P < 0.05$ vs. control PE, $^{\#}P < 0.05$ vs. control PE). (C) ELISA-based activity assay for measuring the kinase activity of mTOR. Recombinant protein blocks dose-dependent mTOR. Immunoprecipitates containing the specified concentrations of PRAS40 or GFP were performed and analyzed by immunoblotting for the indicated proteins. (*D*) Immunoblot showing that PRAS40 blocks activation of mTORC1–S6K1 pathway in NRCMs in response to PE. (*E*) Immunoblot showing that PRAS40TA blocks activation of mTORC1–S6K1 pathway in NRCMs in response to PE.

whereas PRAS40-treated animals showed stabilization of cardiac function and chamber diameter starting at 4 wk after banding. Superior heart function in PRAS40 animals was confirmed by hemodynamic measurement 8 wk after surgery (Fig. 5*B*). Chronic mTORC1 activation results in decreased mTORC2 signaling (5) that might be rescued by PRAS40 overexpression. Indeed, PRAS40-treated mice showed increased phosphorylated Akt (pAKT) levels and increased insulin Receptor Substrate–1 (IRS-1) expression 8 wk after TAC (Fig. 5*C*). Control animals showed signs of congestive heart failure with increased lung weight/body weight ratio (LW/BW), which was prevented in PRAS40-treated mice (Fig. 5*D*). PRAS40 overexpression led to reduced molecular markers of hypertrophy (Fig. 5*E*) and fibrosis (Fig. S3*E*). Importantly, exposure to pressure overload was similar, as the pressure across the aorta was not statistically different among the groups of mice subjected to TAC (Fig. S3*F*). Taken together these data support the idea that PRAS40 can block pathological remodeling and protect cardiac function after TAC, even when injected after initiation of pathological hypertrophy.

PRAS40 Does Not Prevent Physiological Growth. Physiological cardiac hypertrophy occurring after chronic exercise training is distinct

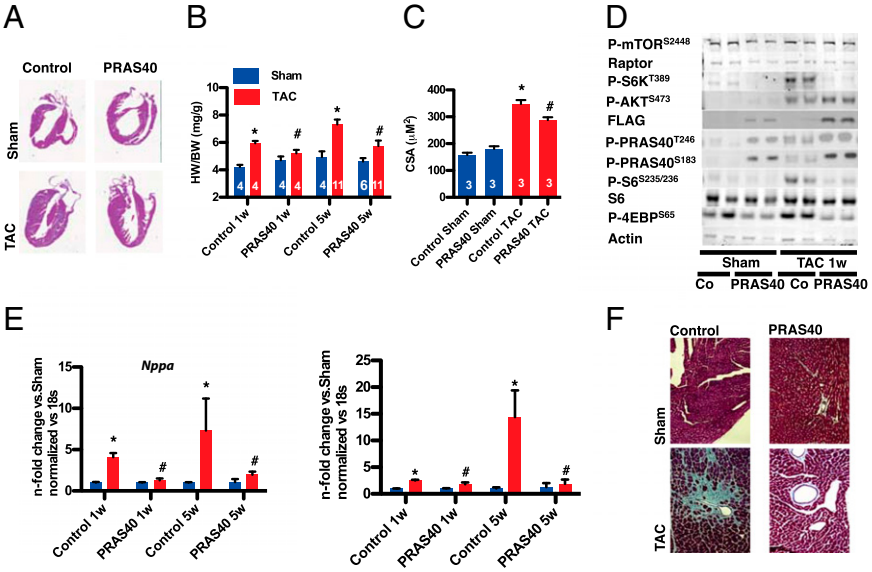

Fig. 3. PRAS40 blocks pathological growth in vivo. (*A*) Gross morphology with H&E staining of either control virus or PRAS40-injected mouse hearts after either sham or TAC surgery in 10-wk-old mice. (*B*) Heart weight (HW) to BW ratio (HW/BW) in control and PRAS40 mice either 1 or 5 wk after sham or TAC surgery. The number of mice per group is indicated within the bar ($^{*}P < 0.01$ versus control sham; $^{\#}P < 0.05$ versus control TAC). (*C*) CSA in control and PRAS40 mice 5 wk after sham or TAC surgery ($^{*}P < 0.01$ versus control sham; $^{\#}P < 0.05$ versus control TAC). (*D*) Immunoblots of whole heart lysates 1 wk after sham or TAC surgery. (*E*) ANP and BNP transcription 1 and 5 wk after sham or TAC surgery ($^{*}P < 0.01$ versus control sham; $^{\#}P < 0.05$ versus control TAC). (*F*) Masson–Trichrome staining from control and PRAS40-treated hearts. Error bars indicate means ± SEM.

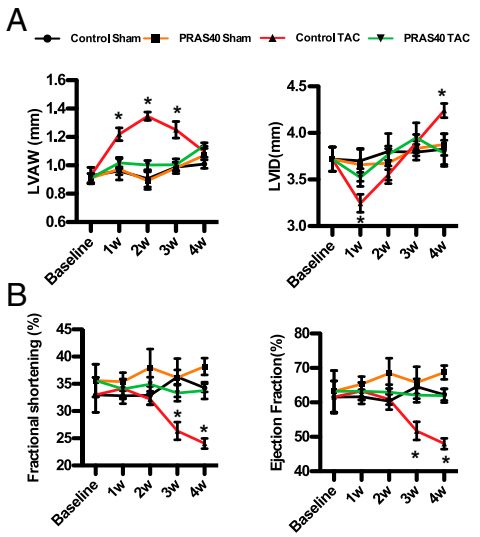

Fig. 4. PRAS40 protects against cardiac dysfunction. (*A*) PRAS40-treated mice (10-wk-old) are resistant to pressure-overload–induced hypertrophy. Line graphs representing weekly echocardiographic assessment of control or PRAS40 sham and TAC-banded hearts for anterior wall dimension (left ventricular wall, LVAW), end-diastolic dimension (left ventricular diameter, LVID), (*B*) percentage of fractional shortening (FS), and ejection fraction (EF) (*$P < 0.05$ vs. control TAC; $n = 4$ per sham and 11 per TAC group). Error bars indicate means ± SEM.

from pathological hypertrophy insofar as being reversible and characterized by normal heart function. Physiological hypertrophy is associated with activation of the phosphatidylinositide 3-kinase (PI3K)–AKT pathway (18, 19), which should strongly promote PRAS40 phosphorylation. Activation of the PI3K–AKT pathway with insulin in NRCM resulted in a small but significant increase in CSA (1.24-fold). Myocytes overexpressing wild-type PRAS40 also responded to insulin with a 1.3-fold increase in cell size (Fig. 6*A*). The ratio of phosphorylated PRAS40–total PRAS40 increased in both control cells and PRAS40-overexpressing NRCMs (Fig. S4*A*). Conversely, rapamycin and PRAS40TA blocked cell size increases, indicating PRAS40 phosphorylation is necessary for physiological growth in vitro. Mechanistically, PRAS40 overexpression inhibited mTOR kinase activity, whereas inhibition of mTOR with PRAS40TA impaired insulin sensitivity (Fig. 6*A*). Less exogenous PRAS40 (detected with the FLAG-tag) was bound to mTOR after treatment with insulin, indicating that sufficient PRAS40 is released from mTORC1 to allow mild physiological growth (Fig. S4*B*). Phosphorylation of RibS6 and 4EBP was not completely blocked by PRAS40 overexpression, whereas the TA mutant completely blocked the phosphorylation (Fig. 6*B*), indicating that strong AKT activation phosphorylates sufficient overexpressed PRAS40 to allow mTORC1 activation. These in vitro findings were confirmed by overexpression of PRAS40 or phospho-dead mutant PRAS40TA with AAV9 in vivo. Physiological hypertrophy can be studied in vivo by a voluntary running wheel experiment. Mild hypertrophy was induced without altering cardiac function as assessed by echocardiography or without increase of hypertrophic gene markers such as ANP (Fig. 6*C* and Fig. S4 *C* and *D*). In agreement with our in vitro data, physiological hypertrophy was not blocked by PRAS40 overexpression, but was inhibited by PRAS40TA (Fig. 6*C*). Exercised mice showed increased AKT phosphorylation compared with sedentary animals (Fig. 6*D*). PRAS40^{T246} phosphorylation that was nearly undetectable in sedentary control mice was markedly increased by exercise in both control mice and PRAS40-overexpressing mice, whereas PRAS40^{S183} phosphorylation remained unchanged. Whereas RibS6 was unphosphorylated in PRAS40 sedentary mice, exercise induced phosphorylation of RibS6 in PRAS40 mice, indicating activation of mTORC1. Raptor expression and mTOR phosphorylation were unaltered after PRAS40 overexpression (Fig. 6*D*), consistent with the in vitro data (Fig. 2*D*). Citrate synthase activity, an index of muscle oxidative capacity and hence physical training, was measured in mixed gastrocnemius muscle of mice that underwent running training to assure that all animals were running to a similar extent (Fig. S4*E*). This supports the idea that phosphorylation of PRAS40 is necessary during physiological hypertrophic growth, as overexpression of a phospho-dead mutant blocks physiological growth, whereas overexpression of wild-type PRAS40 does not prevent physiological hypertrophy, because AKT phosphorylates sufficient PRAS40 to allow activation of mTORC1.

Discussion

mTORC1 is activated in various cardiac diseases including myocardial infarction, hypertrophic growth, genetic cardiomyopathies, and diabetic cardiomyopathies, and rapamycin treatment improves cardiac function in experimental murine cardiomyopathic models. However, chronic administration of rapamycin exhibits systemic side effects, whereas PRAS40 can be delivered to target mTORC1 specifically in myocytes. Selective inhibition of mTORC1 in cardiomyocytes protects myocardium from pathological remodeling via manipulation of PRAS40. Therefore, PRAS40 represents a unique molecular tool to inhibit pathological remodeling.

PRAS40 initially identified as a 14–3–3 binding protein (14) was subsequently found to serve as an mTORC1 inhibitor (8, 9). Nutrients and growth stimuli result in phosphorylation of PRAS40, leading to dissociation of PRAS40 from the complex and relieving

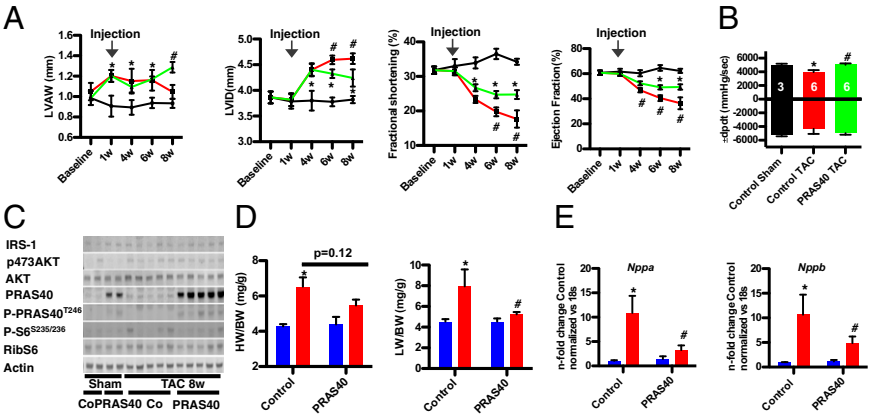

Fig. 5. PRAS40 prevents deterioration of cardiac failure after pressure overload. (*A*) Before injection of PRAS40 or control AAV, echocardiography was performed on each group of mice (10-wk-old). Line graphs representing serial echocardiographic assessment of sham and TAC-banded hearts for LVAW, LVID, FS, and EF (*$P < 0.05$ vs. control, $^{\#}P < 0.05$ vs. control TAC). (*B*) In vivo hemodynamic assessment of control and PRAS40 hearts 8 wk after sham or TAC operation (*$P < 0.05$ versus control sham; $^{\#}P < 0.05$ versus control TAC). (*C*) Immunoblots of whole hearts 8 wk after TAC. (*D*) HW/BW and LW/BW in mice 8 wk after surgery (*$P < 0.01$ versus control sham; $^{\#}P < 0.05$ versus control TAC). (*E*) Nppa and Nppb transcription 8 wk after surgery (*$P < 0.01$ versus control sham; $^{\#}P < 0.05$ versus control TAC). Error bars indicate means ± SEM.

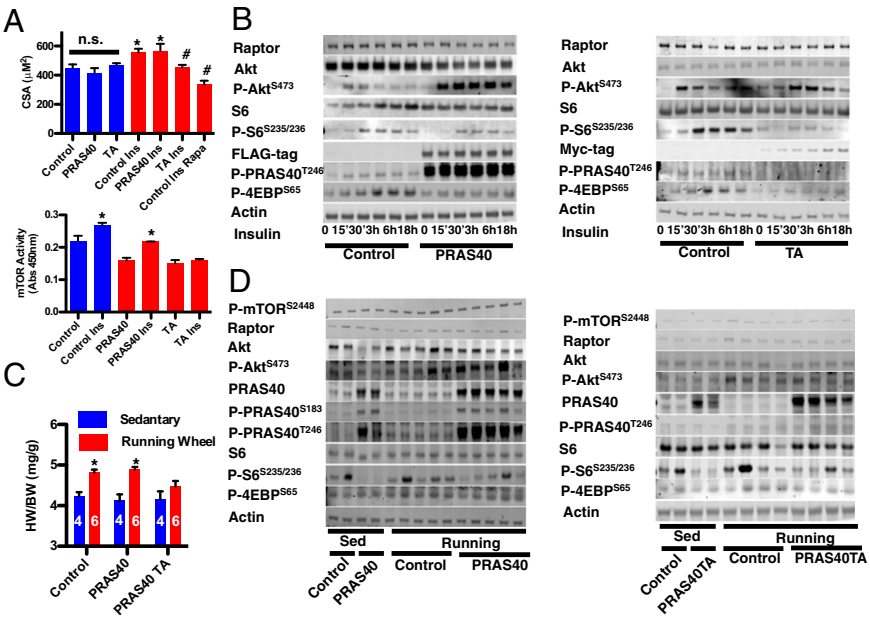

Fig. 6. PRAS40 overexpression allows physiological growth. (*A*, *Upper*) CSA measurements from control, PRAS40, PRAS40TA-infected, or rapamycin-treated (20 nM) NRCMs treated and untreated with insulin (100 nM for 24 h) ($n = 4$ independent experiments, $^{*}P < 0.05$ vs. control; $^{\#}P < 0.05$ versus control Ins). (*A*, *Lower*) ELISA-based activity assay for measuring the kinase activity of mTOR. PRAS40 overexpression blocks mTOR activity. Ins, insulin. (*B*) Cell lysates of control, PRAS40, and PRAS40TA overexpressing myocytes were analyzed by immunoblotting for the levels of the indicated proteins and phosphorylation states. (*C*) HW/BW in control, PRAS40, and PRAS40TA mice (14-wk-old) after 4 wk of exercise. (*D*) Immunoblot of whole heart lysates of the indicated groups 4 wk after sedentary and exercise. Exercise increase of AKT and PRAS40^{T246} phosphorylation. Error bars indicate means ± SEM.

inhibitory constraint. Consistent with findings in noncardiac cells (9, 10), PRAS40 blocks cellular growth in myocytes by inhibition of mTORC1 (Fig. 2). Interestingly, PRAS40 expression also increases in human failing hearts, suggestive of compensation for ongoing hypertrophic growth stimuli. However, knockdown of PRAS40 does not increase cellular growth at baseline conditions, but sensitizes myocytes to growth stimuli with PE. In addition, we cannot rule out the possibility that PRAS40 may influence cell growth by an alternate mechanism independent of mTOR. We have recently initiated creation of PRAS40 null mice to further understand the roles of PRAS40 in cardiac development and growth, which will be the subject of further studies.

Cardiac remodeling during pathological hypertrophic growth is not adaptive in the long term, and clinical studies support beneficial effects of inhibiting chronic remodeling (20–22). Therefore, maladaptive responses have often been targeted with a remarkable number of possible therapeutic targets for treatment of cardiac diseases. However, development of new drugs for heart failure with depressed heart function (with the possible exception of the bradycardic agent ivrabradine) (23) and for patients with heart failure with preserved function (22) have not readily translated from bench to bedside. Most existing therapies target outside–in signaling in cardiac cells, but are limited in effectiveness. Consequently, targeting intracellular signaling might have better therapeutic potential than existing therapies. Recent advancements in the development of AAV vectors resulted in the first clinical trial with AAV-based cardiac gene transfers (24, 25) and manipulation of sarcoplamic reticulum calcium ATPase (SERCA2a) activity improves cardiac function after TAC (26). AAV-mediated gene therapy represents a unique approach to treat and prevent pathological hypertrophy (27, 28). Gene therapy with cardiac-specific expression of PRAS40 completely prevented pathological hypertrophy and ventricular remodeling after TAC, preventing deterioration of cardiac function when injected after surgery, a time point where systolic function is still preserved, but hypertrophy is initiated. Because protein expression following AAV-based gene delivery takes 2–3 wk, initial chamber dilatation and hypertrophy was not repressed, whereas treatment with rapamycin in a former study blocked hypertrophy after TAC (1).

The PI3K–AKT signaling pathway is a critical mediator of physiological hypertrophy (19). The results show that AKT activation during exercise is sufficient to release enough PRAS40 from mTORC1 to allow mild physiological growth. Corroborating evidence showed that overexpression of a phospho-dead mutant PRAS40 blocked physiological hypertrophy, indicating that phosphorylation of PRAS40 is necessary for physiological growth.

Collectively, the results indicate that PRAS40 is a potent and critical mediator of cardioprotection. Effects of PRAS40 were tested in two relevant models, demonstrating that selective mTORC1 inhibition with PRAS40 is a unique therapeutic option to prevent chronic pathological remodeling. Given that hyperactivation of mTORC1 also occurs in diabetic and aging hearts, future studies will focus on whether PRAS40 is also beneficial in other cardiac diseases. Studying PRAS40 biology in the myocardium will potentially reveal unique ways to treat molecular signaling in high-impact research areas including response to pathologic injury, repair, survival, and age-related cardiac dysfunction.

Materials and Methods

Mice, Surgery, and Cardiac Function Analysis. All experiments were performed in 2-d- to 52-wk-old male C57BL/6 mice unless otherwise indicated. Seven-week-old male C57BL/6 mice were purchased from Jackson Labs. Tail vein injection of either control AAV, PRAS40 AAV, or PRAS40TA were performed at 7 wk of age. At 10 wk of age, male mice underwent TAC (TAC model) or a sham operation as previously described (29, 30). A voluntary running regimen was conducted for 4 wk, as previously described (31). For echocardiography, mice were anesthetized with 2% (vol/vol) isoflurane and scanned using a Vevo770 imaging system (Visual Sonics), as previously described (32). Closed chest hemodynamic assessment was performed on anesthetized mice (33). For in vivo injection of insulin, we injected mice i.p. with PBS or insulin (1 U/kg per BW for 1 h) after overnight starvation. Approval from the San Diego State University Institutional Animal Care and Use Committee was obtained for all animal studies.

Isolation and Primary Culture of Neonatal and Adult Ventricular Cardiomyocytes. Isolation and primary culture of neonatal and adult ventricular cardiomyocytes were prepared by standard procedures. Cells were treated with 100 μM PE or insulin (100 nM) for indicated time points. For analysis of hypertrophy, cells were treated with PE or insulin for 24 h.

Adenoviral Constructs and siRNA. To generate recombinant adenoviruses, the human and mutated human PRAS40 cDNAs were subcloned into the pShuttle–CMV vector using the AdEasy XL Adenoviral Vector system (Stratagene) as previously described, with additional details provided in *SI Text* (29).

AAV9 Generation and Systemic in Vivo AAV9 Cardiac-Targeted Gene Transfer Protocol. In vivo cardiac-targeted PRAS40 expression in normal mouse hearts was obtained by using tail vein injection of an AAV9 harboring the PRAS40

CELL BIOLOGY

gene or PRAS40TA mutant driven by a cardiomyocyte-specific CMV–MLC2v0.8 promoter as previously described (34).

Sample Preparation, Immunoblotting, RT-PCR, and Immunoprecipitation. Whole-heart, isolated myocytes and human heart lysates were prepared as described previously, with additional details provided in *SI Text* (29). Immunoblots from isolated cells or tissue were conducted as previously described (30). A complete list of antibodies and primers is provided in Tables S3 and S4. RNA was isolated using the Quick RNA MiniPrep kit (ZymoResearch) according to the manufacturer's protocol. We generated cDNA and carried out real-time PCR using the cDNA preparation kit and SYBR real-time PCR (Biorad) according to the manufacturer's protocol. We calculated differences using the $\Delta\Delta C(T)$ method. Immunoprecipitation of mTOR and PRAS40 was carried out as described below using a previously published protocol (8). PRAS40 or GFP cDNAs were transfected into HeLa cells and the proteins purified using immobilized FLAG-antibody resin. Proteins were eluted from the resin with 50 mg/mL FLAG peptide and stored on ice until use. In the experiments using recombinant protein, PRAS40 or GFP was incubated for 30 min to the precipitated mTORC before measuring the mTOR kinase activity.

mTOR Kinase Activity Assay. mTOR kinase activity was measured with the K-LISA mTOR Activity Kit (EMD–Millipore), whicht uses a p70S6K–GST fusion protein as a specific mTOR substrate using the manufacturer's protocol.

Histology and Staining. Immunocytochemistriy was performed using standard procedures, with additional details provided in *SI Text*. Sections were cut and deparaffinized using standard procedures. Immunostaining on paraffin-embedded hearts was performed as described previously in detail (35). Sections were also used to visualize cardiomyocyte cell membrane by staining with tetramethyl rhodamine isothiocyanate–conjugated wheat-germ agglutinin (Sigma-Aldrich).

PLA. PLAs to detect protein–protein interactions in situ were performed as previously described (36).

Measurement of Citrate Synthase Activity. Citrate synthase activity in skeletal muscle was measured using the Citrat Synthase ELISA kit (Abcam) using the manufacturer's protocol.

Statistical Analysis. Statistical analysis was performed using Student *t* test, and ANOVA as appropriate, with Tukey or Bonferroni post hoc tests. All data were analyzed with GraphPad Prism 5.0 (Graphpad Software Inc.; P values < 0.05 were considered significant).

ACKNOWLEDGMENTS. We thank all members of the M.A.S. laboratory for helpful discussion and comments. This study was supported by National Institutes of Health grants to M.A.S. and C.C.G.; Deutsche Forschungsgemeinschaft (DFG) 1659/1-1 (to M.V.) and 3900/1-1 (to M.H.K.); The Rees-Stealy Research Foundation (to S. Doroudgar, P.Q., and S. Din); and the San Diego Chapter of the Achievement Rewards for College Scientists Foundation, the American Heart Association Predoctoral Fellowship 10PRE3410005, and the Inamori Foundation (to S. Doroudgar).

1. McMullen JR, et al. (2004) Inhibition of mTOR signaling with rapamycin regresses established cardiac hypertrophy induced by pressure overload. *Circulation* 109(24): 3050–3055.
2. Buss SJ, et al. (2009) Beneficial effects of mammalian target of rapamycin inhibition on left ventricular remodeling after myocardial infarction. *J Am Coll Cardiol* 54(25): 2435–2446.
3. Marin TM, et al. (2011) Rapamycin reverses hypertrophic cardiomyopathy in a mouse model of LEOPARD syndrome-associated PTPN11 mutation. *J Clin Invest* 121(3):1026–1043.
4. Paoletti E, Cannella G (2009) Reducing the risk of left ventricular hypertrophy in kidney transplant recipients: The potential role of mammalian target of rapamycin. *Transplant Proc* 41(6, Suppl):S3–S5.
5. Laplante M, Sabatini DM (2012) mTOR signaling in growth control and disease. *Cell* 149(2):274–293.
6. Zoncu R, Efeyan A, Sabatini DM (2011) mTOR: From growth signal integration to cancer, diabetes and ageing. *Nat Rev Mol Cell Biol* 12(1):21–35.
7. Sengupta S, Peterson TR, Sabatini DM (2010) Regulation of the mTOR complex 1 pathway by nutrients, growth factors, and stress. *Mol Cell* 40(2):310–322.
8. Sancak Y, et al. (2007) PRAS40 is an insulin-regulated inhibitor of the mTORC1 protein kinase. *Mol Cell* 25(6):903–915.
9. Vander Haar E, Lee SI, Bandhakavi S, Griffin TJ, Kim DH (2007) Insulin signalling to mTOR mediated by the Akt/PKB substrate PRAS40. *Nat Cell Biol* 9(3):316–323.
10. Fonseca BD, Smith EM, Lee VH, MacKintosh C, Proud CG (2007) PRAS40 is a target for mammalian target of rapamycin complex 1 and is required for signaling downstream of this complex. *J Biol Chem* 282(34):24514–24524.
11. Oshiro N, et al. (2007) The proline-rich Akt substrate of 40 kDa (PRAS40) is a physiological substrate of mammalian target of rapamycin complex 1. *J Biol Chem* 282(28): 20329–20339.
12. Wang L, Harris TE, Roth RA, Lawrence JCJ, Jr. (2007) PRAS40 regulates mTORC1 kinase activity by functioning as a direct inhibitor of substrate binding. *J Biol Chem* 282(27): 20036–20044.
13. Wiza C, Nascimento EBM, Ouwens DM (2012) Role of PRAS40 in Akt and mTOR signaling in health and disease. *AJP: Endocrinology and Metabolism* 302(12):E1453–E1460.
14. Kovacina KS, et al. (2003) Identification of a proline-rich Akt substrate as a 14-3-3 binding partner. *J Biol Chem* 278(12):10189–10194.
15. Beausoleil SA, et al. (2004) Large-scale characterization of HeLa cell nuclear phosphoproteins. *Proc Natl Acad Sci USA* 101(33):12130–12135.
16. Nascimento EB, et al. (2006) Insulin-mediated phosphorylation of the proline-rich Akt substrate PRAS40 is impaired in insulin target tissues of high-fat diet-fed rats. *Diabetes* 55(12):3221–3228.
17. Fonseca BD, Lee VH-Y, Proud CG (2008) The binding of PRAS40 to 14-3-3 proteins is not required for activation of mTORC1 signalling by phorbol esters/ERK. *Biochem J* 411(1):141–149.
18. McMullen JR, et al. (2003) Phosphoinositide 3-kinase(p110alpha) plays a critical role for the induction of physiological, but not pathological, cardiac hypertrophy. *Proc Natl Acad Sci USA* 100(21):12355–12360.
19. Bernardo BC, Weeks KL, Pretorius L, McMullen JR (2010) Molecular distinction between physiological and pathological cardiac hypertrophy: Experimental findings and therapeutic strategies. *Pharmacol Ther* 128(1):191–227.
20. Frey N, Katus HA, Olson EN, Hill JA (2004) Hypertrophy of the heart: A new therapeutic target? *Circulation* 109(13):1580–1589.
21. Esposito G, et al. (2002) Genetic alterations that inhibit in vivo pressure-overload hypertrophy prevent cardiac dysfunction despite increased wall stress. *Circulation* 105(1):85–92.
22. McKinsey TA, Kass DA (2007) Small-molecule therapies for cardiac hypertrophy: Moving beneath the cell surface. *Nat Rev Drug Discov* 6(8):617–635.
23. Shah AM, Mann DL (2011) In search of new therapeutic targets and strategies for heart failure: Recent advances in basic science. *Lancet* 378(9792):704–712.
24. Pacak CA, Byrne BJ (2011) AAV vectors for cardiac gene transfer: Experimental tools and clinical opportunities. *Mol Ther* 19(9):1582–1590.
25. Jaski BE, et al.; Calcium Up-Regulation by Percutaneous Administration of Gene Therapy In Cardiac Disease (CUPID) Trial Investigators (2009) Calcium upregulation by percutaneous administration of gene therapy in cardiac disease (CUPID Trial), a first-in-human phase 1/2 clinical trial. *J Card Fail* 15(3):171–181.
26. Kho C, et al. (2011) SUMO1-dependent modulation of SERCA2a in heart failure. *Nature* 477(7366):601–605.
27. Belke DD, Gloss B, Swanson EA, Dillmann WH (2007) Adeno-associated virus-mediated expression of thyroid hormone receptor isoforms-alpha1 and -beta1 improves contractile function in pressure overload-induced cardiac hypertrophy. *Endocrinology* 148(6):2870–2877.
28. Sakata S, et al. (2007) Restoration of mechanical and energetic function in failing aortic-banded rat hearts by gene transfer of calcium cycling proteins. *J Mol Cell Cardiol* 42(4):852–861.
29. Muraski JA, et al. (2007) Pim-1 regulates cardiomyocyte survival downstream of Akt. *Nat Med* 13(12):1467–1475.
30. Muraski JA, et al. (2008) Pim-1 kinase antagonizes aspects of myocardial hypertrophy and compensation to pathological pressure overload. *Proc Natl Acad Sci USA* 105(37):13889–13894.
31. Carraway MS, et al. (2010) Erythropoietin activates mitochondrial biogenesis and couples red cell mass to mitochondrial mass in the heart. *Circ Res* 106(11):1722–1730.
32. Quijada P, et al. (2012) Preservation of myocardial structure is enhanced by Pim-1 engineering of bone marrow cells. *Circulation Research* 111(1):77–86.
33. Fischer KM, et al. (2011) Cardiac progenitor cell commitment is inhibited by nuclear Akt expression. *Circ Res* 108(8):960–970.
34. Völkers M, et al. (2011) The inotropic peptide βARKct improves βAR responsiveness in normal and failing cardiomyocytes through G($\beta\gamma$)-mediated L-type calcium current disinhibition. *Circ Res* 108(1):27–39.
35. Avitabile D, et al. (2011) Nucleolar stress is an early response to myocardial damage involving nucleolar proteins nucleostemin and nucleophosmin. *Proc Natl Acad Sci USA* 108(15):6145–6150.
36. Völkers M, et al. (2012) Orai1 deficiency leads to heart failure and skeletal myopathy in zebrafish. *J Cell Sci* 125(Pt 2):287–294.

Supporting Information

Völkers et al. 10.1073/pnas.1301455110

SI Text

Voluntary Exercise. Mice were supplied ad libitum with food and water and housed individually in cages containing rodent exercise wheels. The system consisted of a 5.356-inch diameter wheel (Model InnoWheel, BioServe) equipped with a digital magnetic counter activated by wheel rotation.

Tissue Collection. We killed mice at various time points after transaortic constriction (TAC), exercise, or sham operation and removed the hearts. For later isolation of RNA and protein in the study, left ventricles were stored in liquid N2.

Retroperfusions. Mice were killed under chloral hydrate sedation. Before the procedure of removing the hearts, mice were weighed in grams. Thereafter, hearts were arrested in diastole by catheterizing the abdominal aorta and flushing the heart with a high-potassium/cadmium solution. Phosphate buffered formalin fixative was perfused into the coronary arteries at systolic pressure, while the left ventricle was filled with formalin at diastolic pressure. Retroperfused hearts were then removed from the chest cavity and placed in formalin for at least 24 h, weighed in milligram, and processed for paraffin embedding.

Paraffin heart sections were deparaffinized in xylene and rehydrated through graded alcohols to distilled water. Antigen retrieval was achieved by boiling the slides in 10 mmol/L citrate pH 6.0 for 12–15 min. Slides were washed several times with distilled water and once with Tris-HCL NaCl buffer (TN) buffer (100 mmol/L Tris, 150 mmol/L NaCl). Endogenous tissue peroxidase activity was quenched with TN buffer supplemented with 3% (vol/vol) H_2O_2 for 20 min whenever necessary. Slides were then washed in TN buffer and blocked in Tris-HCL NaCl blocking buffer (TNB) buffer (TSATM kit from Perkin-Elmer) at room temperature for at least 30 min. Primary antibodies were applied overnight at 4 °C in TNB buffer. The next day, samples were washed in TN buffer and incubated with secondary antibodies at room temperature in the dark for 2 h. When amplification of signal was needed, slides were washed in TN buffer and incubated with streptavidin horseradish peroxidase-conjugated diluted 1:100 vol/vol in TNB buffer for 30 min at room temperature, and signals were developed using Tyramide substrate diluted 1:50 vol/vol in Amplification Diluent (Perkin-Elmer) for 10 min. Slides were washed in TN buffer and coverslipped using Vectashield eventually in the presence of DNA staining. List of primary and secondary antibodies is reported in Table S3.

Immunohistochemistry. Immunostaining of myocytes was performed on cells grown on permanox or glass chamber slides (gelatin-coated). Cells were fixed by 4% paraformaldehyde (PFA) for 20 min at room temperature, permeabilized in PBS supplemented by 0.1% Triton-X for 10 min, and blocked in PBS supplemented with 10% horse serum for at least 30 min. Before starting the protocol and at the end of each successive step, cells were washed in PBS at room temperature. Primary antibodies diluted in blocking solution (PBS with 10% horse serum) were applied overnight at 4 °C. The next day, cells were washed with PBS and incubated for 1 h at room temperature and in the dark, with the secondary antibody (Jackson Laboratories) diluted in blocking solution. Conjugated phalloidin 633 (Jackson Laboratories) was diluted in the same buffer at 1:100 vol/vol. Sytox Blue or To-Pro (Molecular Probes) was diluted in Vectashield (Vectra Labs) mounting media at 1:500 vol/vol and used as nuclear staining.

Adenoviral Constructs and siRNA. The human full-length of Proline Rich AKT Substrate of 40 kDa (PRAS40) contained a C-terminal FLAG tag, the threonine to alanine (TA) mutant a C-terminal myc tag. Neonatal rat cardiomyocytes and adult myocytes were infected with adenoviruses as described previously at a multiplicity of infection of 20 (1). To down-regulate PRAS40 in rat neonatal cardiomyocytes, we transfected cells with PRAS40-specific siRNA (Ambion) or a negative- control siRNA (Ambion) at a final concentration of 25 nM with HiPerfect (Quiagen).

Sample Preparation, Immunoblotting, and RT-PCR. Immunoblots from isolated cells or tissue were conducted as previously described (1–3). RNA were isolated using the Quick RNA MiniPrep kit (ZymoResearch) according to the manufacturer's protocol. We generated cDNA and carried out real-time PCR using the cDNA preparation kit and SYBR real-time PCR (Biorad) according to the manufacturer's protocol. We calculated differences using the ΔΔC (T) method. A full list of primers and antibodies is provided in Tables S3 and S4.

Radiolabeled Amino Acid Incorporation Assay. Cells were plated at 1.0 × 106 cells per well in a six-well plastic culture dish in DMEM/F-12 containing 10% FBS. Twenty-four hours after plating, cultures were treated and incubated with 1 μCi/mL 3H-phenylalanine (Perkin-Elmer Cat. No. NET1122001MC; 1 mCi/mL, 110 Ci/mmol) in DMEM/F-12 containing 2% FBS for 6 h. The media were then removed, the cultures were washed twice with PBS, and 700 μL of 10% trichloroacetic acid were added to each well. The culture plates were then frozen at –20 °C, thawed at room temperature, and then scraped. To each sample 100 μL of 0.5 mg/mL BSA were added, and precipitated proteins were collected by centrifugation at 9,600 × *g* for 15 min at 4 °C. The acid-soluble fraction was then removed, and 200 μL of solubilization buffer (1% TritonX-100, 1 M NaOH) were added to each sample, and samples were incubated at room temperature for 1 h. A portion of each sample (180 μL) was added to glass scintillation vials containing 10 mL scintillation fluid and counted using one counting cycle with 2-min count time and no sigma coincidence. Results are expressed as disintegrations per minute (DPMs).

Immunoprecipitation. Immunoprecipitation of mechanistic target of rapamycin (mTOR) and PRAS40 was carried out as described below using a previously published protocol (4). Cell cultures or whole heart lysates were prepared in ice-cold nondenaturating lysis buffer (40 mM Hepes pH 7.4, 2 mM EDTA, 10 mM pyrophosphate, 10 mM glycerophosphate, 0.3% CHAPS). After brief centrifugation (13,000 × *g*, 4 °C for 5 min), pellets were resuspended in 200 μL lysis buffer, incubated for 30 min at 4 °C, and centrifuged (13.000 rcf, 4 °C for 15 min). Supernatants were diluted to 1 μg/1 μL protein with lysis buffer and rotated with BSA-treated A/G-PLUS-Agarose (20 mL/500 mL; Santa Cruz Biotechnology sc-2003) for 4 h and centrifuged at 13.000 rcf for 15 min at 4 °C to remove protein nonspecifically bound to A/G-Agarose. The supernatants were then mixed with precipitating antibodies for mTOR or subtype-matched control IgGs and rotated for 8 h at 4 °C. Again, A/G-PLUS-Agarose was added, and samples were rotated for an additional 4 h and centrifuged (13.000 rcf, room temperature for 15 min). Pellets were washed three times with lysis buffer, and 50 μL lysis buffer supplemented with mercaptoethanol (2% vol/vol) was added. Samples were heated at 95 °C for 1 min and centrifuged (800 rcf, room temperature for

15 min). Proteins were resolved with SDS/PAGE electrophoresis and subjected to immunoblotting.

Adeno-Associated Virus Serotype 9 Generation and Systemic in Vivo AAV9 Cardiac-Targeted Gene Transfer Protocol. We obtained CMV–myosin light chain (MLC) 0.26–PRAS40 by replacing the enhanced green fluorescent protein (EGFP) cDNA of pdsAAVCMV–MLC0.26–EGFP with human PRAS40 (GenBank accession no. NM_032375.3). High-titer vectors were produced with a triple transfection approach of 293T cells in cell stacks as described before (5). For production of adeno-associated virus serotype 9 (AAV9)–PRAS40 and PRAS40TA, p5E18–VD2–9 providing the AAV-9 cap sequence and cytomegalovirus (CMV)-Rep52/40 expression construct (pDGdelVP) containing adenoviral helper sequences were cotransfected with pdsAAVCMV–MLC0.26–PRAS40. Subsequently, vectors were harvested after 48 h, purified by filtration cascade (first 5 μm, second 0.8 μm, third 0.2 μm) and Iodixanol step gradient centrifugation, and quantitated using real-time PCR as reported before. pdsCMV–MLC0.26–EMPTY was used to generate an analogous control vector. Adult male C57/B6 mice (age 7 wk) were anesthetized with isoflurane (2%). We injected 100 μL of 37 °C heated PBS containing either 1×1011 total viral particles of either AAV9–Control ($n = 40$) or AAV9–PRAS40 and AAV9–PRAS40TA into the circulation via the tail vein using a 28G1/2 insulin syringe. After injections, animals remained in a supervised setting until fully conscious and were observed for an additional 6 h. Animals were inspected daily for a period of 6 wk after systemic gene transfer. The gene transfer protocol caused neither death nor damage to animals enrolled in the study and resulted in homogenous in vivo cardiomyocyte transduction. All viruses are available upon request.

1. Cheng Z, et al. (2011) Mitochondrial translocation of Nur77 mediates cardiomyocyte apoptosis. *Eur Heart J* 32(17):2179–2188.
2. Most P, et al. (2004) Cardiac adenoviral S100A1 gene delivery rescues failing myocardium. *J Clin Invest* 114(11):1550–1563.
3. Muraski JA, et al. (2008) Pim-1 kinase antagonizes aspects of myocardial hypertrophy and compensation to pathological pressure overload. *Proc Natl Acad Sci USA* 105(37):13889–13894.
4. Sancak Y, et al. (2007) PRAS40 is an insulin-regulated inhibitor of the mTORC1 protein kinase. *Mol Cell* 25(6):903–915.
5. Völkers M, et al. (2011) The inotropic peptide βARKct improves βAR responsiveness in normal and failing cardiomyocytes through G(βγ)-mediated L-type calcium current disinhibition. *Circ Res* 108(1):27–39.

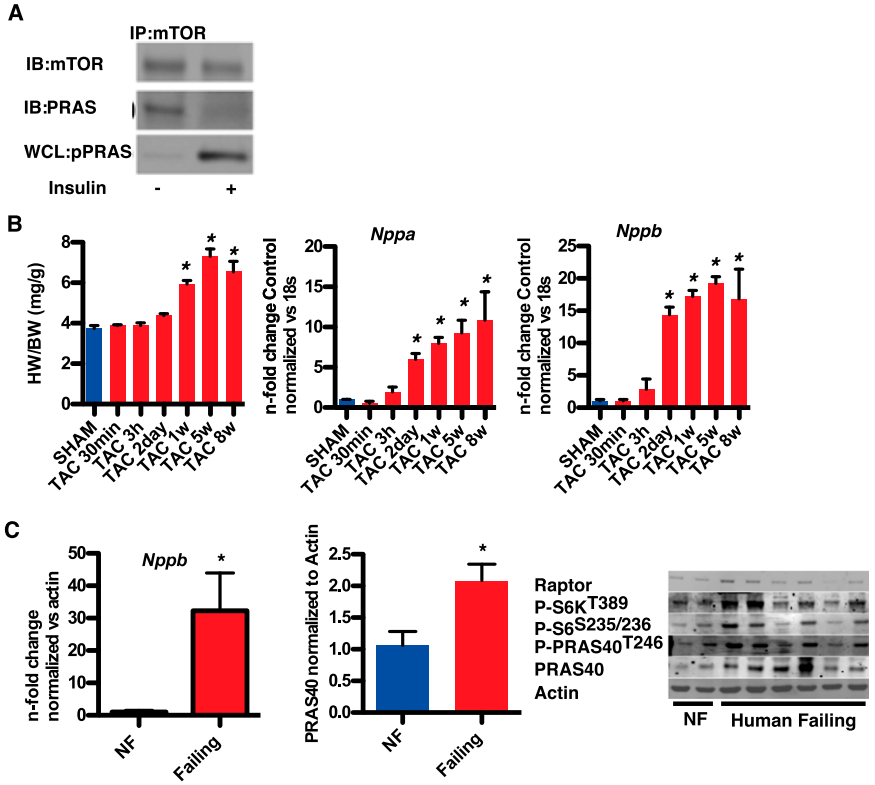

Fig. S1. (*A*) Immunoprecipitation against mTOR and immunoblots for mTOR and PRAS40 with and without insulin (100 nM for 1 h). (*B*) Heart weight/body weigth ratio (HW/BW) after TAC time course and gene expression of atrial natriuretic factor (ANP) and brain natriuretic factor (BNP) (*$P < 0.05$ vs. sham, $n = 3$ for each time point). (*C*) Immunoblotting of normal and failing human hearts for PRAS40. BNP transcription in human failing hearts ($P < 0.05$ vs. nonfailing). Bar graph for PRAS40 expression in human failing hearts.

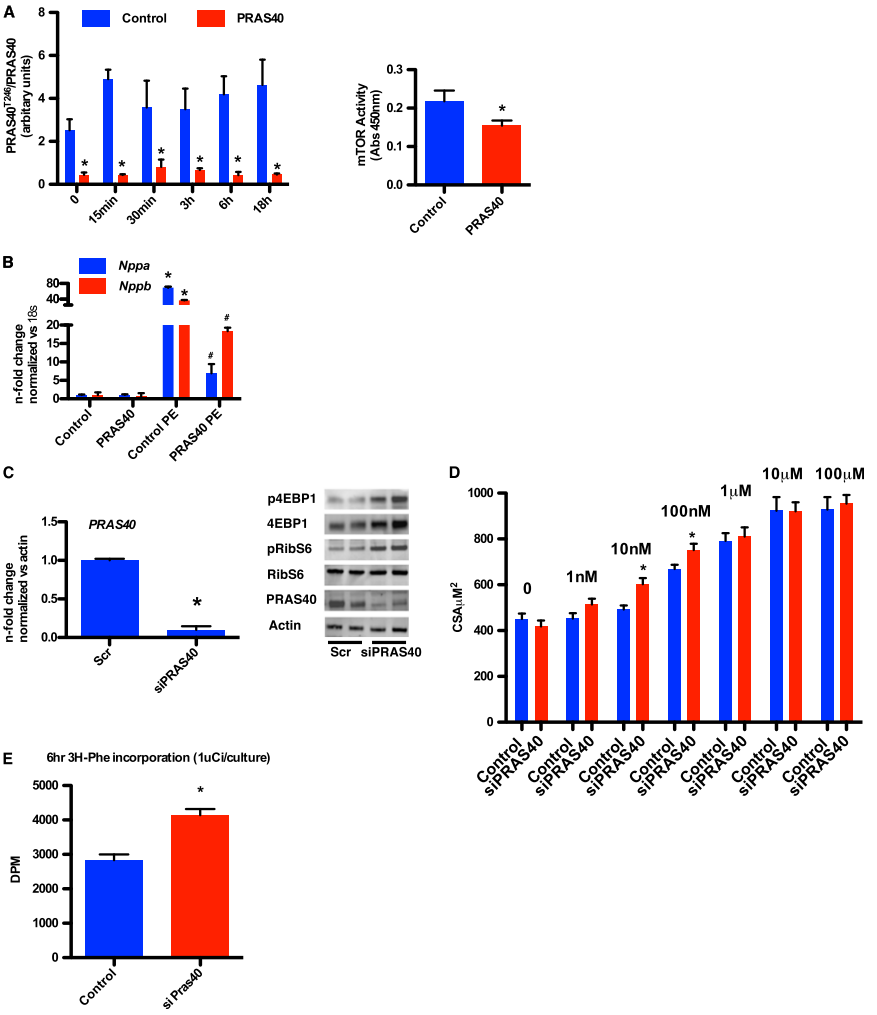

Fig. S2. (*A*) Quantitation of the phosphorylated PRAS40–total PRAS40 ratio after treatment with phenylephrine for the indicated time points. ELISA-based activity assay for measuring the kinase activity of mTOR. Overexpressed PRAS40 protein blocks mTOR activity. $^{*}P < 0.05$ vs. control. (*B*) qRT-PCR of molecular markers of hypertrophy in NRCMs infected with control or PRAS40 treated and untreated with PE. Fold change compared with control represented ($^{*}P < 0.05$ vs. control, $^{\#}P < 0.05$ vs. control PE). (*C*) Knockdown of PRAS40 activates mTORC1. NRCMs were transfected with siRNA against PRAS40. Cell lysates after 48 h were analyzed by immunoblotting for the levels of the indicated proteins and phosphorylation states. (*D*) Cell surface area from control siRNA or siPRAS40 transfected neonatal rat cardiomyocyte cultures treated and untreated with PE with indicated concentrations for 24 h. ($n = 2$ independent experiments). Error bars indicate means ± SEM. (*E*) 3H-Phenylalanine incorporation after PRAS40 silencing. $^{*}P < 0.05$ vs. control.

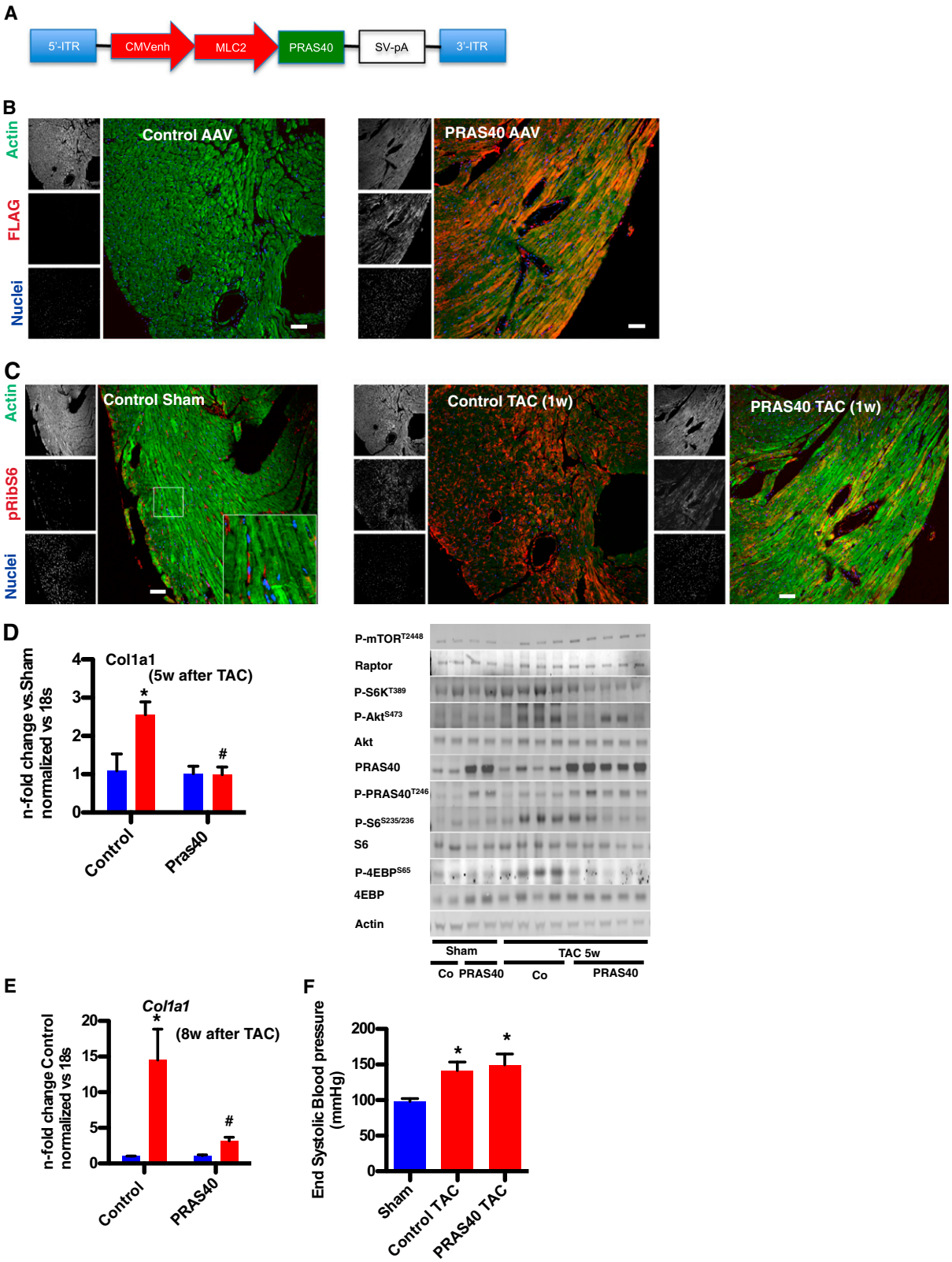

Fig. S3. (*A*) Scheme of the AAV9PRAS40 under MLC2 promoter to overexpress PRAS40 in myocytes. (*B*) Immunohistochemistry confirms robust overexpression of the FLAG-tag. Representative confocal scans are shown for FLAG, actin, and nuclei (red, green, and blue, respectively, in overlays). (*B*) Confocal microscopy of paraffin-embedded sections from control and PRAS40 mouse hearts after sham or TAC surgery (1 wk) stained for phospho–Ribosomal S6 (RibS6) (red), Actin (green), and nuclei (blue). RibS6 is highly phosphorylated in control hearts after TAC. (Scale bar, 150 μm.) (*C*) Immunoblot of whole heart lysates of the indicated groups 5 wk after sham and TAC surgery. (*D*) qPCR measurement of collagen transcription in control or PRAS40-treated animals 5 wk after sham and TAC. (*E*) qPCR measurement of collagen transcription in control or PRAS40-treated animals 8 wk after sham and TAC surgery. (*F*) In vivo measurement of systolic blood pressure after TAC surgery (*$P < 0.05$ vs. sham).

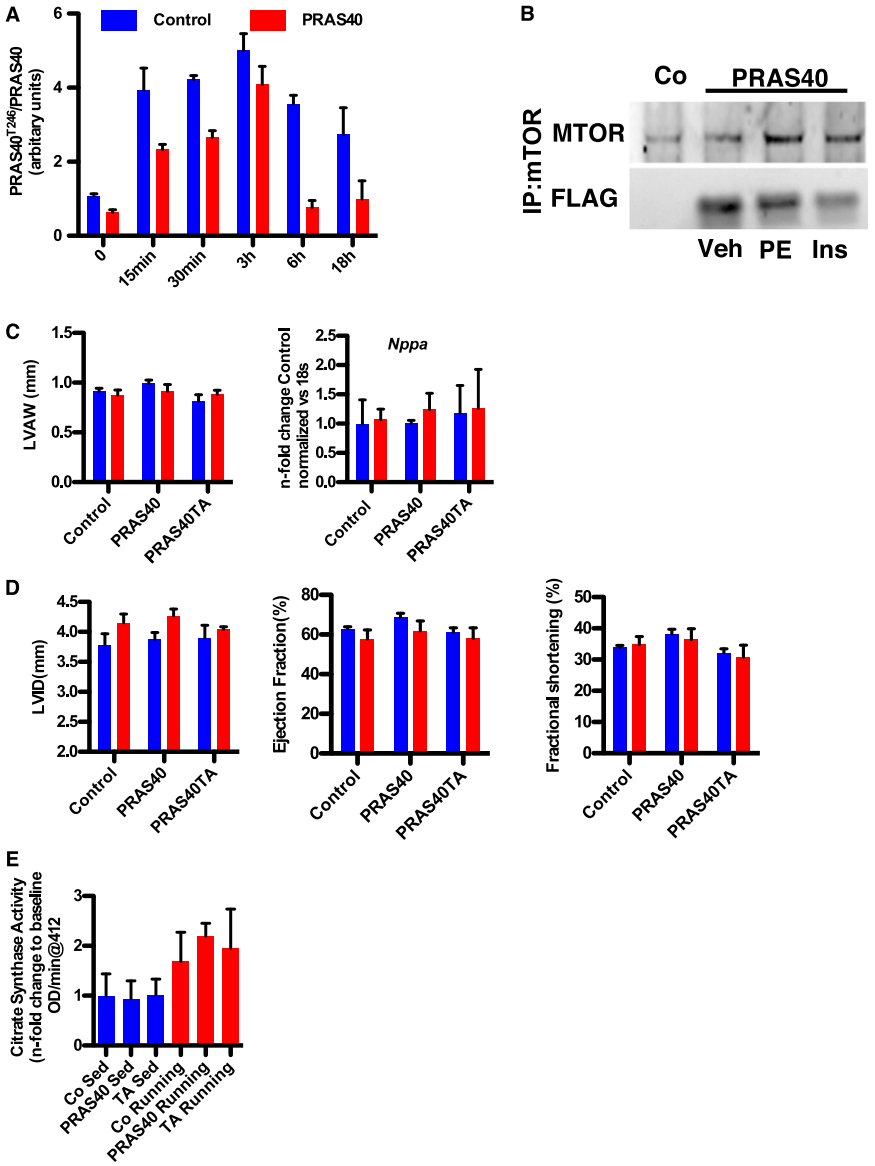

Fig. S4. (*A*) Quantitation of the phosphorylated PRAS40–total PRAS40 ratio after treatment with insulin for the indicated time points. (*B*) Immunoprecipitation against mTOR and immunoblots for FLAG after indicated treatments. Less exogenous PRAS40 is bound to mTOR after insulin (100 nM for 1 h). (*C*) Echocardiographic assessment of control or PRAS40 sedentary and exercised hearts for left ventricular wall (LVAW) (n = 4 sham and 6 exercise group). ANP transcription in hearts of mice of the indicated group 4 wk after exercise. (*D*) Echocardiographic assessment of control or PRAS40 sedentary and exercised hearts for left ventricular diameter (LVID) (n = 4 sham and 6 exercise group). Echocardiographic assessment of control or PRAS40 sedentary and exercised hearts for ejection fraction (EF) and fractional shortening (FS). (*E*) Activity of citrate synthase in gastrocenimus muscle in sedentary or exercised mice.

Table S1. Characterization of mice after sham or TAC by morphometry and echocardiography 1 wk after surgery

	Sham		TAC	
1 wk after surgery	Control $n = 10$	PRAS40 $n = 6$	Control $n = 15$	PRAS40 $n = 15$
LVAW, mm	0.9610 ± 0.02	0.9720 ± 0.07	1.219 ± 0.04*	1.017 ± 0.03#
LVPW, mm	0.9580 ± 0.07	0.9680 ± 0.09	1.381 ± 0.04*	1.100 ± 0.07#
LVID,mm	3.609 ± 0.13	3.506 ± 0.21	3.245 ± 0.09*	3.521 ± 0.09#
LVIS,mm	2.640 ± 0.14	2.696 ± 0.22	2.461 ± 0.15*	2.709 ± 0.10#
FS, %	32.81 ± 1.44	35.39 ± 1.65	34.14 ± 1.67	34.05 ± 1.83
EF,%	61.56 ± 4.66	63.21 ± 6.04	63.28 ± 4.67	63.25 ± 2.54
HR, bpm	443 ± 20	452 ± 8	466 ± 14	454 ± 16
HW/BW, mg/g; $n = 4$	4.22 ± 0.15	4.69 ± 0.28	5.94 ± 0.25*	5.2 ± 0.19#

EF, %, ejection fraction; FS, %, fractional shortening; HR, bpm, heart rate; HW/BW, heart weight/body weight ratio; LVID, mm, left ventricular end-diastolic dimensions; LVIS, mm, left ventricular end-systolic dimensions; LVPW, mm, left ventricular posterior wall dimensions; LVAW, mm, left ventricular anterior wall dimensions; *n*, number of mice analyzed. *$P < 0.05$ vs. control sham; #$P < 0.05$ vs. control TAC.

Table S2. Characterization of mice after sham or TAC by morphometry and echocardiography 5 wk after surgery

	Sham		TAC	
5 wk after surgery	Control $n = 4$	PRAS40 $n = 6$	Control $n = 11$	PRAS40 $n = 11$
BW				
LVAW, mm	0.9178 ± 0.03	0.9900 ± 0.03	1.096 ± 0.04	1.013 ± 0.04
LVPW, mm	0.9278 ± 0.07	0.9400 ± 0.07	0.9782 ± 0.06	1.014 ± 0.05
LVID, mm	3.826 ± 0.14	3.875 ± 0.11	4.134 ± 0.08*	3.781 ± 0.05#
LVIS, mm	2.833 ± 0.09	2.823 ± 0.18	3.399 ± 0.12*	2.7770.13#
FS, %	34.27 ± 1.35	38.20 ± 1.54	24.05 ± 0.94*	33.75 ± 1.53#
EF,%	62.24 ± 1.64	68.71 ± 1.99	48.01 ± 1.99*	61.96 ± 2.00#
HR, bpm	459 ± 16	436 ± 19	457 ± 14	491 ± 15
HW/BW, mg/g	4.93 ± 0.42	4.61 ± 0.25	7.31 ± 0.35*	5.74 ± 0.40#

BW, body weight. *$P < 0.05$ vs. control sham; #$P < 0.05$ vs. control TAC.

Table S3. Primer table

18s forward	5′-CGAGCCGCCTGGATACC-3′
18s reverse	5′-CATGGCCTCAGTTCCGAAAA-3′
ANP forward	5′-TGGGTCTTGTTAGGGCTCAAACCT-3′
ANP reverse	5′-TGAAACTCAAGGGACACCCATCGT-3′
BNP forward	5′-AATGGCCCAGAGACAGCTCTTGAA-3′
BNP reverse	5′-CTTGTGCCCAAAGCAGCTTGAGAT-3′
mPRAS40 forward	5′-CGGAGAGCACAGACGACGGC-3′
mPRAS40 reverse	5′-GCACCGACACGGGCAGAGAC-3′
hPRAS40 forward	5′-TCACCGTCGCGAGAAAGCGG-3′
hPRAS40 reverse	5′-GCGACCTGACGTCCCTGACC-3′
Collagen 1a1 forward	5′-AAGACGGGAGGGCGAGTGCT-3′
Collagen 1a1 reverse	5′-TCTCACCGGGCAGACCTCGG-3′

Table S4. Antibody table

Application	Antibody	Dilution	Amplify	Company
Immunoblot	Actin	1:2,000	No	Santa Cruz (sc-81178)
Immunoblot	p246PRAS40	1:1,000	No	CST (#2640)
Immunoblot	PRAS40	1:1,000	No	CST (#2691)
Immunoblot	pS6Rib	1:2,000	No	CST (#4857)
Immunoblot	RibS6	1:500	No	CST (#2317)
Immunoblot	p473AKT	1:1,000	No	CST (#4058)
Immunoblot	p389S6K	1:500	No	CST (#9234)
Immunoblot	IRS-1	1:1,000	No	CST (#2390)
Immunoblot	p389S6K	1:500	No	CST (#9205)
Immunoblot	AKT	1:2,000	No	CST (#2966)
IHC	α-Sarcomeric actin	1:100	No	Sigma (A2172)
IHC	p246PRAS40	1:100	Yes	CST (#2640)
IHC	pS6Rib	1:100	Yes	CST (#4857)
IHC	FLAG	1:100	Yes	Sigma (F3165)

CST, cell signaling technology; IHC, immunohistochemistry; IRS-1, Insulin Receptor Substrate–1.